13th ewtec 2019 Proceedings of the 13th European Wave and Tidal Energy Conference 1-6 Sept 2019, Naples, Italy

Wave farm effects on coastal flooding under climate change

Rafael J. Bergillos, Cristobal Rodriguez-Delgado, and Gregorio Iglesias

Abstract—**The objective of this work is to investigate whether a wave farm, i.e., an array of wave energy converters, can provide protection from flooding on the coast in its lee under climate change through a case study: a gravel-dominated beach in southern Spain (Playa Granada). We consider three sea level rise (SLR) scenarios: the present situation (SLR0), an optimistic projection (SLR1) and a pessimistic projection (SLR2). Two state-of-the-art numerical models, SWAN and XBeach-G, are applied to determine the wave propagation patterns, total run-up and flooded dry beach area. The results indicate that the absorption of wave power by the wave farm affects wave propagation in its lee and, in particular, wave heights, with alongshore-averaged reductions in breaking wave heights about 10% (25%) under westerly (easterly) storms. These lower significant wave heights, in turn, result in alongshore-averaged run-up reductions for the three scenarios. The dry beach area flooded under westerly (easterly) storms is also reduced by 5.7% (3.2%), 3.3% (4.9%) and 1.99% (4.5%) in scenarios SLR0, SLR1 and SLR2, respectively. These findings prove that a wave farm can actually reduce coastal flooding on its leeward coast.**

Keywords—**Climate change, coastal defence, coastal flooding, sea level rise, wave energy**

I. Introduction

OVER the past few decades, the demand for energy worldwide has grown massively and has been mainly met by fossil fuels [1]–[3].

ID: 1263. Track: Environmental impact and appraisal. This work was supported by the research grants WAVEIMPACT (PCIG-13-GA-2013-618556, European Commission) and ICE (Contract no. 5025, European Commission,). RB was partly funded by the University of Granada (Programa Contratos Puente 2017) and the Spanish Ministry of Science, Innovation and Universities (research contract FJCI-2017-31781). Wave, sea-level rise, bathymetric and DEM data were provided by Puertos del Estado (Spain), Universität Hamburg (Germany), Ministerio de Agricultura, Pesca y Alimentación (Spain), and Instituto Geográfico Nacional (Spain), respectively.

R. J. Bergillos is with Hydraulic Engineering Area, Department of Agronomy, University of Cordoba, Rabanales Campus, Leonardo da Vinci Building, 14071 Cordoba, Spain (e-mail: rafael.bergillos@uco.es).

C. Rodriguez-Delgado is at PROES consultores, 28020, Madrid, Spain (e-mail: crodriguez@proes.engineering).

G. Iglesias is at MaREI, Environmental Research Institute & School of Engineering, University College Cork, College Road, Cork, Ireland (e-mail: gregorio.iglesias@ucc.ie).

However, these fossil fuels induce acute damage to the environment and contribute to aggravate the negative consequences of climate change [4], [5]. Thus, the development and usage of carbon-free energy sources are increasingly necessary [6]. Wave energy is, among the renewable sources of energy, one of the most advisable due to its huge availability and potential [7], [8], and its relatively low impacts on the environment with respect to other carbon-free energy sources [9], [10].

Notable progress on wave energy has been achieved recently along the following research lines: (i) the characterization of the wave energy resource [11]–[18]; (ii) the development and improvement of different types of wave energy technologies [19]–[26]; (iii) the analysis of potentially viable locations [27]–[29]; (iv) the joint assessment of wave and other renewable energy sources [30]–[33] and (v) the study of economic indicators [34]–[37].

Wave farms, i.e., arrays of wave energy converters (WECs), have been proven to be capable of performing the dual function of generating carbon-free energy and protecting sandy coastlines against erosion [38]–[43]. Recent works have also demonstrated that wave farms mitigate erosion issues on mixed and gravel-dominated coasts [44]–[47]. The dual function of wave farms can contribute to the development of wave energy, given that many coasts across the world are experiencing erosion issues due to direct human intervention [48], [49], and climate change [50]. However, the impacts of wave farms on coastal flooding considering the effects of sea-level rise (SLR) have not been fully addressed so far.

The overall objective of this work is to investigate the influence of a wave farm on significant wave height at breaking, total run-up (including water level) and flooded area under three SLR scenarios: the present situation (SLR0), and optimistic (SLR1) and pessimistic (SLR2) projections proposed by [51]. For this purpose, a wave model (SWAN) and a storm response model (XBeach-G) were jointly applied to two case studies (with and without wave farm) under storm conditions. The study area, Playa Granada (Fig. 1), is a gravel-dominated beach that is experiencing terminal erosion and coastal flooding issues [52]–[57].

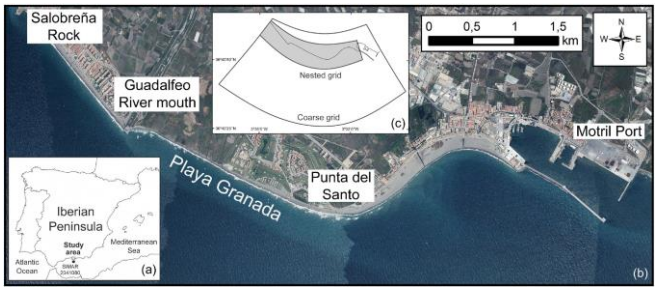

Fig. 1. (a) Location of the study area in southern Spain, (b) plan view of the deltaic coast, indicating the studied stretch of beach (Playa Granada), (c) contours of the numerical grids used in the SWAN model. (Source: [58]. Reproduced with permission of Elsevier).

II. METHODS

A. Wave farm location and geometry

In order to analyse the effects of a wave farm on wave propagation and coastal flooding, we selected the wave farm location indicated in Fig. 2, with the geometrical centre situated at 30 m water depth. This position was found to be optimum in terms of both wave energy availability [29] and coastline protection [46].

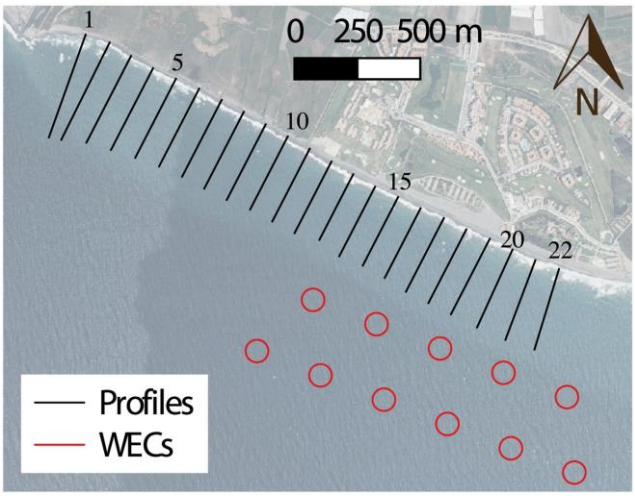

Fig. 2. Location of the studied beach profiles (1–22, in black) and wave energy converter farm (in red). (Source: [58]. Reproduced with permission of Elsevier).

The wave farm layout consisted of eleven WaveCat WECs, distributed in two rows and with an inter-device spacing equal to 180 m (Fig. 2). WaveCat is a type of overtopping WEC composed by two hulls connected by the stern, with a distance between them commonly equal to 90 m [59]. The efficiency of WaveCat and the wave farm layout selected for coastal defence purposes has been widely demonstrated in previous works (e.g. [45] and [47]).

B. Sea states and sea level rise scenarios

The effects of western and eastern storms (prevailing wave directions at the study site) were simulated by means of the SWAN and XBeach-G models. The input wave conditions for SWAN were deep-water significant wave height equal to 3.1 m, spectral peak period equal to 8.4 s (the most common value at the study area for storm conditions) and deep-water wave directions equal to 238° (107°) for the westerly (easterly) storm. These are the most frequent wave directions at the study site under western and eastern storm conditions, respectively. These sea states were modelled under high tide conditions and for a storm surge of 0.5 m (typical value in the study area under storm conditions).

These storms were modelled for two case studies and three SLR scenarios. The two study cases correspond to the natural, no-farm situation (i.e., baseline case study) and the situation including the wave farm described in Section II.1 (i.e., wave farm case study).

On the other hand, the three tested SLR scenarios were: present situation (SLR0) and SLR associated to the representative concentration pathways 4.5 and 8.5 at the study area according to [51], which represent optimistic (SLR1=0.45 m) and pessimistic (SLR2=0.65 m) projections by 2100, respectively.

C. SWAN model

The spectral wave model SWAN [60] was used to propagate the two storm sea states from deep water to the nearshore region under the three SLR scenarios described in the previous section. The SWAN model was validated for the study area by means of comparison with hydrodynamic measurements collected by two ADCPs during a continuous 41-day field survey [61]. In this work, we used the computational grids shown in Fig. 1c, which were also employed for the calibration of the model.

The WaveCat devices were modelled in SWAN as artificial obstacles. The adopted values of the reflection and transmission coefficients were 0.43 and 0.76, respectively, according to those measured for this type of WEC during laboratory experiments by [21]. The results of the SWAN model were used to quantify the variations in breaking wave height values induced by the presence of the wave farm. They were also employed to provide the input conditions for the XBeach-G model, as detailed in the following section.

D. XBeach-G model

The storm impact model XBeach-G, which was specifically developed for reproducing the storm hydrodynamics, hydrology and morphodynamics of gravel-dominated beaches [61], [62], was applied to quantify the values of the total run-up (including water level) under the storm conditions and sea-level rise scenarios detailed in Section II.2. The XBeach-G model was validated for the study area by means of comparison with morphological data measured before and after storm events [63], [64].

The XBeach-G model was applied to 22 equally-spaced beach profiles (one per 100 m) along the stretch of beach studied (Fig. 2). The offshore boundary conditions for XBeach-G were computed based on the results of

SWAN along the 10 m contour for all the beach profiles. This value of the offshore depth is in agreement with all the model requirements [65]. On the other hand, the land-side boundaries were variables alongshore depending on the type of land use located landward of the beach profiles (farming settlements, hotel complex, golf field or residential properties, see Fig. 2).

The results of the XBeach-G model were employed to compute the maximum values of total run-up and flooded cross-shore distance in every beach profile. The values of total flooded area along the section of Playa Granada for the study cases and SLR scenarios considered were also obtained.

III. RESULTS

E. Significant wave heights at breaking

Under westerly storms, the presence of the wave farm leads to a reduction in the breaking wave height in the eastern part of Playa Granada (Fig. 3). The reduction peak values are equal to 24.1% (SLR0), 26.4% (SLR1) and 25.8% (SLR2), whereas the alongshore-averaged reductions in Playa Granada are 9.3%, 9.8% and 9.9%, respectively. Conversely, in the west side of the farm, the significant wave height at breaking of the wave farm case study is slightly increased with respect to the baseline (Fig. 3 a1–b1). This is influenced by the reflection and diffraction processes induced by the devices.

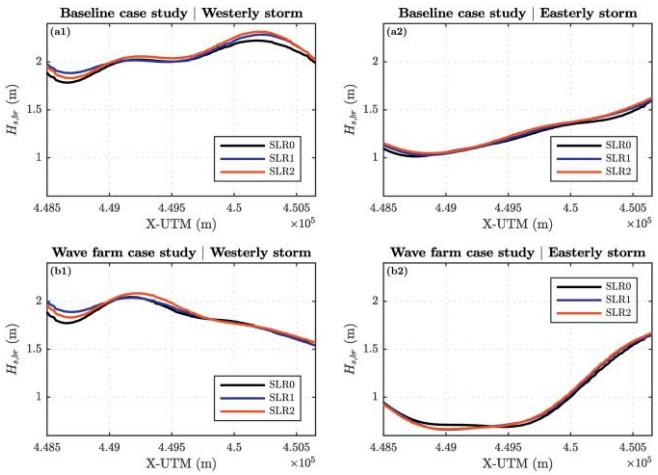

Fig. 3. Significant wave height at breaking along the studied stretch of beach for the baseline (a) and wave farm (b) case studies under westerly (1) and easterly (2) storms. Scenarios SLR0, SLR1 and SLR2. (Source: [58]. Reproduced with permission of Elsevier).

Under eastern storm conditions, the reductions in significant wave height are concentrated in the western part of Playa Granada, and extend along a greater distance than under westerly storms, with maximum reductions of up to 42%, 40.3% and 41.9% for scenarios SLR0, SLR1 and SLR2, respectively. In this case, increases in wave height values are observed to the east of the wave farm location, also influenced by the WEC-induced diffraction and reflection processes (Fig. 3 a2–b2). Under these wave conditions, the alongshore-averaged reductions induced by the farm in scenarios SLR0, SLR1 and SLR2 are equal to 24.8%, 25.7% and 26.3%, respectively.

In both case studies and for both wave directions, it is observed that, in general, the greater the SLR, the greater the breaking significant wave heights. Thus, climate change will not only induce SLR, but these variations in sea level will also lead to greater wave height and power in the breaking zone. Both the SLR and the increase in breaking wave height will contribute to coastal flooding, as explained below.

F. Total run-up

Under western storms, the wave farm reduces the total run-up, from profile 12 to profile 22, up to 14.1%, 8.7% and 8.3% in scenarios SLR0, SLR1 and SLR2, respectively. The alongshore-averaged reductions in total run-up along the studied stretch of beach for scenarios SLR0, SLR1 and SLR2 are equal to 5.9%, 2.6% and 1.5%, respectively. Thus, the reductions are more significant in scenario SLR0 than those in scenarios SLR1 and SLR2 (Figs. 4 and 5). The total run-up in the wave farm case study is slightly increased with respect to the baseline in the western part of Playa Granada. This is influenced by the greater breaking significant wave heights at this location for the wave farm case (Fig. 3).

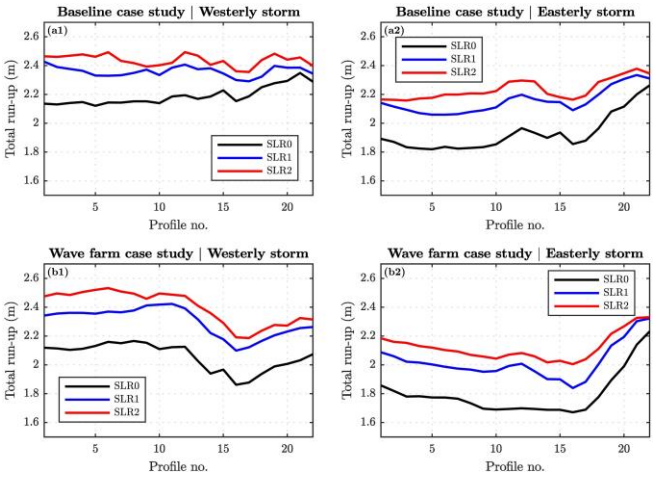

Fig. 4. Total run-up values in the studied beach profiles for the baseline (a) and wave farm (b) case studies under westerly (1) and easterly (2) storms. Scenarios SLR0, SLR1 and SLR2. (Source: [58]. Reproduced with permission of Elsevier).

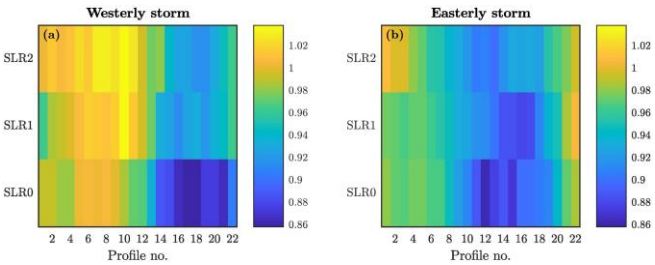

Fig. 5. Ratio of total run-up for the wave farm case study with respect to the baseline under westerly (a) and easterly (b) storms. Scenarios SLR0, SLR1 and SLR2. (Source: [58]. Reproduced with permission of Elsevier).

Under eastern storm conditions, the total run-up is reduced due to the presence of the wave farm along most of the stretch of beach considered, with only some minor increases in its eastern boundary (Figs. 4 and 5). The farm leads to maximum (alongshore-averaged) reductions in total run-up of 13.6% (6.8%), 12% (6.1%) and 10.1% (5.1%) for scenarios SLR0, SLR1 and SLR2, respectively. Under these wave conditions, the total run-up values are generally lower than those under western storms. This is due to the orientation of the coastline in Playa Granada, which is almost normal to the prevailing western direction under high energy conditions.

The results for all the wave conditions, study cases and SLR scenarios detailed in this section highlight the efficiency of wave farms composed by WaveCat WECs for the reduction of total run-up values. This has important implications for the mitigation of coastal flooding events, as it is detailed in the following sections.

G. Flooded cross-shore distances

This section reports the flooded cross-shore distances for the wave conditions, study cases and SLR scenarios analyzed. These flooded distances, which are influenced by both the total run-up values depicted in Fig. 4 and the morphologies of the emerged beach profiles, are shown in Fig. 6.

For westerly storms, reductions in flooded distances occur between profiles 11 and 22 in scenario SLR0, and between profiles 17 and 22 in scenarios SLR1 and SLR2 (Fig. 7). This is influenced by the SLR values in scenarios SLR1 and SLR2, which lead to an overwash of the whole beach for the case studies with and without wave farm in profiles 1–16. The maximum (alongshore-averaged) reductions in flooded cross-shore distances induced by the wave farm under western storm conditions for scenarios SLR0, SLR1 and SLR2 are equal to 16.2% (4.8%), 15.7% (2.5%) and 10.1% (1.5%), respectively.

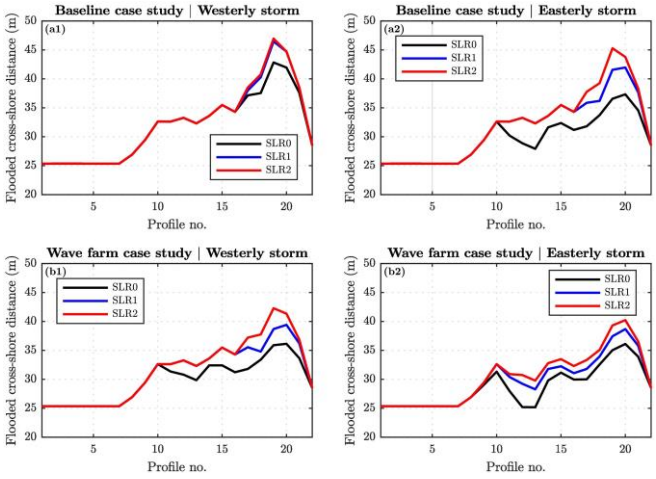

Fig. 6. Flooded cross-shore distances in the studied beach profiles for the baseline (a) and wave farm (b) case studies under westerly (1) and easterly (2) storms. Scenarios SLR0, SLR1 and SLR2. (Source: [58]. Reproduced with permission of Elsevier).

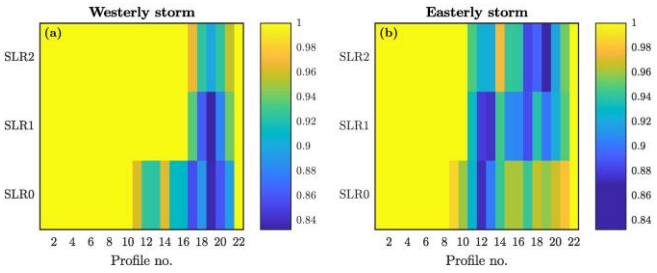

Fig. 7. Ratio of flooded cross-shore distance for the wave farm case study with respect to the baseline under westerly (a) and easterly (b) storms. Scenarios SLR0, SLR1 and SLR2. (Source: [58]. Reproduced with permission of Elsevier).

Under easterly storms, the flooded distance diminishes due to the wave farm in profiles 11 to 21 for the three SLR scenarios (Figs. 6 and 7). In profiles 1 to 10, the beach is overwashed in each scenario in the same way as for westerly storms. This is due to the lower dry beach area in this stretch, which is closer to the river mouth and has experienced greater values of shoreline retreat in recent years due to river regulation. For eastern storm conditions, the maximum (alongshore-averaged) farm-induced reductions in flooded cross-shore distances in scenarios SLR0, SLR1 and SLR2 are equal to 11.8% (3.1%), 12.5% (4.4%) and 12.2% (3.8%), respectively. The reductions for these wave conditions are extended along the whole urbanized stretch of beach, with maximum values of 6 m; whereas under westerly storms the reductions are concentrated in the eastern part of Playa Granada, reaching values up to 7.8 m (Fig. 6).

H. Flooded area

Fig. 8 represents the total flooded dry beach areas in the baseline and wave farm study cases for the three SLR scenarios under both western and eastern storm conditions. Under westerly storms, the reductions in coastal flooding induced by the wave farm are equal to 3976.4 m² (5.7%), 2331.5 m² (3.3%) and 1404.1 m² (1.99%) for scenarios SLR0, SLR1 and SLR2, respectively. Thus, the reduction in flooded area decreases with increasing SLR values. This trend is influenced by the SLR-induced overwash of the whole dry beach in both study cases for scenarios SLR1 and SLR2 at some locations that are not overwashed for scenario SLR0 (profiles 11–16, see Figs. 6 and 7). In any case, the wave farm provides protection against flooding in all the SLR scenarios.

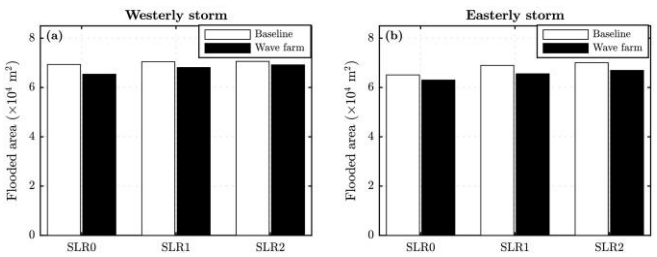

Fig. 8. Total flooded area in the baseline and wave farm case studies for scenarios SLR0, SLR1 and SLR2 under westerly (a) and easterly (b) storms. (Source: [58]. Reproduced with permission of Elsevier).

For eastern storm conditions, the differences in flooded dry beach area between the baseline and wave farm case studies in scenarios SLR0, SLR1 and SLR2 are equal to 2095.3 m^2 (3.2%), 3419.4 m^2 (4.9%) and 3155.5 m^2 (4.5%), respectively. The maximum reduction takes place in scenario SLR1 since some parts of the beach are only fully overwashed in both study cases for scenario SLR2, reducing the farm-induced differences in flooded dry beach area for this latter scenario.

In scenarios SLR1 and SLR2, the reductions are significantly greater under easterly storms, so that a wave farm would be particularly helpful to reduce the flooded areas associated to the IPCC projections for these wave conditions. Under both wave directions, the coastal flooding increases with increasing values of SLR for both study cases, being the flooded area in the wave farm case study lower than in the baseline for all the SLR scenarios. Thus, these results indicate that a wave farm would contribute to mitigate coastal flooding issues in Playa Granada, which will be more severe in the coming years due to the expected SLR induced by climate change.

IV. CONCLUSIONS

This work has investigated the efficiency of a wave farm in reducing storm-induced coastal flooding on a gravel-dominated beach under three sea-level rise scenarios: present situation (SLR0), optimistic projection (SLR1) and pessimistic projection (SLR2). With this purpose, the SWAN and XBeach-G models, previously validated for the study site, were coupled and applied to 22 beach profiles in order to assess significant wave heights at breaking, total run-up values (including water level), flooded cross-shore distances and total flooded area for the prevailing storm directions (SW and SE) and the three aforementioned SLR scenarios. The results were compared to the baseline (no farm) case study.

In terms of wave propagation patterns, under westerly storms, the WEC farm modifies significantly the wave height leeward of the devices and leads to a reduction in significant wave height at breaking in the eastern part of the study area. Conversely, the reductions in breaking wave height under easterly storms extend along most of the study area, reaching the maximum reduction values in the western part. The breaking significant wave heights are slightly increased with respect to the baseline to the west (east) of the wave farm under westerly (easterly) storms. This is due to the wave diffraction and reflection processes induced by the WECs.

The total run-up is reduced in the central and eastern parts of the beach under western storms; whereas under eastern storm conditions the total run-up decreases along most of the study area, with total run-up values generally lower than those under western storms. This is explained by the shoreline orientation in Playa Granada, which is almost normal to the incoming westerly waves. The total run-up is also slightly increased with respect to the baseline under westerly (easterly) storm waves in the western (eastern) part of the beach, induced by the greater breaking significant wave heights at these locations for the wave farm case.

Finally, flooded cross-shore distances are also reduced by the farm along the studied coastline section for both wave directions. The farm-induced decreases in flooded dry beach area under westerly (easterly) storms are equal to 5.7% (3.2%), 3.3% (4.9%) and 1.99% (4.5%) in scenarios SLR0, SLR1 and SLR2, respectively. These results highlight the potential of wave farms to mitigate coastal flooding, alongside their primary function of carbon-free energy generation. Further research is required to investigate the wave farm effects on the shoreline evolution and dry beach area availability due to changes in wave propagation and longshore sediment transport under sea-level rise.

REFERENCES

[1] M. Asif, T. Muneer, Energy supply, its demand and security issues for developed and emerging economies, Renewable and Sustainable Energy Reviews 11 (2007) 1388-1413.

[2] S. Shafiee, E. Topal, When will fossil fuel reserves be diminished?, Energy policy 37 (2009) 181-189.

[3] C. Gaete-Morales, A. Gallego-Schmid, L. Stamford, A. Azapagic, Assessing the environmental sustainability of electricity generation in Chile, Science of The Total Environment 636 (2018) 1155-1170.

[4] B. Atilgan, A. Azapagic, Life cycle environmental impacts of electricity from fossil fuels in Turkey, Journal of Cleaner Production 106 (2015) 555-564.

[5] T. Feng, W. Zhou, S. Wu, Z. Niu, P. Cheng, X. Xiong, G. Li, Simulations of summertime fossil fuel CO 2 in the Guanzhong basin, China, Science of The Total Environment 624 (2018) 1163-1170.

[6] European Commission, A European Strategic Energy Technology Plan (Set-Plan): Towards a low carbon future, Brussels: Commission of the European Communities (2007).

[7] A. M. Cornett, A global wave energy resource assessment, in: The Eighteenth International Offshore and Polar Engineering Conference, International Society of Offshore and Polar Engineers, 2008.

[8] J. Cruz, Ocean wave energy: current status and future perspectives, Springer Science & Business Media, 2008.

[9] A. Clément, P. McCullen, A. F. de O. Falçao, A. Fiorentino, F. Gardner, K. Hammarlund, G. Lemonis, T. Lewis, K. Nielsen, S. Petroncini, M.-T. Pontes, P. Schild, B.-O. Sjöström, H. C. Sørensen, T. Thorpe, Wave energy in Europe: current status and perspectives, Renewable and Sustainable Energy Reviews 6 (2002) 405-431.

[10] A. Palha, L. Mendes, C. J. Fortes, A. Brito-Melo, A. Sarmento, The impact of wave energy farms in the shoreline wave climate: Portuguese pilot zone case study using Pelamis energy wave devices, Renewable Energy 35 (2010) 62-77.

[11] G. Iglesias, R. Carballo, Choosing the site for the first wave farm in a region: A case study in the Galician Southwest (Spain), Energy 36 (2011) 5525-5531.

[12] R. Carballo, M. Sánchez, V. Ramos, J. Fraguela, G. Iglesias, The intraannual variability in the performance of wave energy converters: A comparative study in N Galicia (Spain), Energy 82 (2015) 138-146.

[13] M. López, M. Veigas, G. Iglesias, On the wave energy resource of Peru, Energy Conversion and Management 90 (2015) 34-40.

[14] D. Silva, A. R. Bento, P. Martinho, C. G. Soares, High resolution local wave energy modelling in the Iberian Peninsula, Energy 91 (2015) 1099-1112.
[15] A. Viviano, S. Naty, E. Foti, T. Bruce, W. Allsop, D. Vicinanza, Largescale experiments on the behaviour of a generalised oscillating water column under random waves, Renewable Energy 99 (2016) 875-887.
[16] E. Medina-López, R. Bergillos, A. Moñino, M. Clavero, M. Ortega-Sánchez, Effects of seabed morphology on oscillating water column wave energy converters, Energy 135 (2017) 659-673.
[17] A. López-Ruiz, R. J. Bergillos, J. M. Raffo-Caballero, M. Ortega-Sánchez, Towards an optimum design of wave energy converter arrays through an integrated approach of life cycle performance and operational capacity, Applied Energy 209 (2018) 20-32.
[18] A. López-Ruiz, R. J. Bergillos, A. Lira-Loarca, M. Ortega Sánchez, A methodology for the long-term simulation and uncertainty analysis of the operational lifetime performance of wave energy converter arrays, Energy 153 (2018) 126-135.
[19] A. F. de O. Falçao, Modelling and control of oscillating-body wave energy converters with hydraulic power take-o_ and gas accumulator, Ocean Engineering 34 (2007) 2021-2032.
[20] L. Margheritini, D. Vicinanza, P. Frigaard, SSG wave energy converter: Design, reliability and hydraulic performance of an innovative overtopping device, Renewable Energy 34 (2009) 1371-1380.
[21] H. Fernandez, G. Iglesias, R. Carballo, A. Castro, J. Fraguela, F. Taveira-Pinto, M. Sanchez, The new wave energy converter WaveCat: Concept and laboratory tests, Marine Structures 29 (2012) 58-70.
[22] I. López, B. Pereiras, F. Castro, G. Iglesias, Optimisation of turbine-induced damping for an OWC wave energy converter using a RANS-VOF numerical model, Applied Energy 127 (2014) 105-114.
[23] I. López, G. Iglesias, Efficiency of OWC wave energy converters: A virtual laboratory, Applied Ocean Research 44 (2014) 63-70.
[24] I. López, B. Pereiras, F. Castro, G. Iglesias, Performance of OWC wave energy converters: Influence of turbine damping and tidal variability, International Journal of Energy Research 39 (2015) 472-483.
[25] I. López, A. Castro, G. Iglesias, Hydrodynamic performance of an oscillating water column wave energy converter by means of particle imaging velocimetry, Energy 83 (2015) 89-103.
[26] P. Contestabile, C. Iuppa, E. Di Lauro, L. Cavallaro, T. L. Andersen, D. Vicinanza, Wave loadings acting on innovative rubble mound breakwater for overtopping wave energy conversion, Coastal Engineering 122 (2017) 60-74.
[27] R. Carballo, M. Sánchez, V. Ramos, F. Taveira-Pinto, G. Iglesias, A high resolution geospatial database for wave energy exploitation, Energy 68 (2014) 572-583.
[28] C. Iuppa, L. Cavallaro, E. Foti, D. Vicinanza, Potential wave energy production by different wave energy converters around Sicily, Journal of Renewable and Sustainable Energy 7 (2015) 061701.
[29] A. López-Ruiz, R. J. Bergillos, M. Ortega-Sánchez, The importance of wave climate forecasting on the decision-making process for nearshore wave energy exploitation, Applied Energy 182 (2016) 191-203.
[30] S. Astariz, G. Iglesias, Enhancing wave energy competitiveness through co-located wind and wave energy farms. A review on the shadow effect, Energies 8 (2015) 7344-7366.
[31] S. Astariz, J. Abanades, C. Perez-Collazo, G. Iglesias, Improving wind farm accessibility for operation and maintenance through a co-located wave farm: Influence of layout and wave climate, Energy Conversion and Management 95 (2015) 229-241.
[32] S. Astariz, G. Iglesias, Output power smoothing and reduced downtime period by combined wind and wave energy farms, Energy 97 (2016) 69-81.
[33] C. Pérez-Collazo, D. Greaves, G. Iglesias, A review of combined wave and offshore wind energy, Renewable and Sustainable Energy Reviews 42 (2015) 141-153.
[34] S. Astariz, G. Iglesias, The economics of wave energy: A review, Renewable and Sustainable Energy Reviews 45 (2015) 397-408.
[35] S. Astariz, A. Vazquez, G. Iglesias, Evaluation and comparison of the levelized cost of tidal, wave, and offshore wind energy, Journal of Renewable and Sustainable Energy 7 (2015) 053112.
[36] S. Astariz, G. Iglesias, Wave energy vs. other energy sources: A reassessment of the economics, International Journal of Green Energy 13 (2016) 747-755.
[37] P. Contestabile, E. Di Lauro, M. Buccino, D. Vicinanza, Economic Assessment of Overtopping BReakwater for Energy Conversion (OBREC): A Case Study in Western Australia, Sustainability 9 (2017).
[38] D. Millar, H. Smith, D. Reeve, Modelling analysis of the sensitivity of shoreline change to a wave farm, Ocean Engineering 34 (2007) 884-901.
[39] E. Mendoza, R. Silva, B. Zanuttigh, E. Angelelli, T. L. Andersen, L. Martinelli, J. Q. H. Nørgaard, P. Ruol, Beach response to wave energy converter farms acting as coastal defence, Coastal Engineering 87 (2014) 97-111.
[40] J. Abanades, D. Greaves, G. Iglesias, Wave farm impact on the beach profile: A case study, Coastal Engineering 86 (2014) 36-44.
[41] J. Abanades, D. Greaves, G. Iglesias, Coastal defence through wave farms, Coastal Engineering 91 (2014) 299-307.
[42] J. Abanades, D. Greaves, G. Iglesias, Coastal defence using wave farms: The role of farm-to-coast distance, Renewable Energy 75 (2015) 572-582.
[43] J. Abanades, G. Flor-Blanco, G. Flor, G. Iglesias, Dual wave farms for energy production and coastal protection, Ocean & Coastal Management 160 (2018) 18-29.
[44] R. J. Bergillos, A. López-Ruiz, E. Medina-López, A. Moñino, M. Ortega-Sánchez, The role of wave energy converter farms on coastal protection in eroding deltas, Guadalfeo, southern Spain, Journal of Cleaner Production 171 (2018) 356-367.
[45] C. Rodriguez-Delgado, R. J. Bergillos, M. Ortega-Sanchez, G. Iglesias, Protection of gravel-dominated coasts through wave farms: Layout and shoreline evolution, Science of The Total Environment 636 (2018) 1541-1552.
[46] C. Rodriguez-Delgado, R. J. Bergillos, M. Ortega-Sánchez, G. Iglesias, Wave farm effects on the coast: The alongshore position, Science of The Total Environment 640 (2018) 1176-1186.
[47] C. Rodriguez-Delgado, R. J. Bergillos, G. Iglesias, Dual wave energy converter farms and coastline dynamics: the role of inter-device spacing, Science of The Total Environment, 646 (2019) 1241-1252.
[48] L. Aragonés, J. Pagán, M. López, J. García-Barba, The impacts of Segura River (Spain) channelization on the coastal seabed, Science of The Total Environment 543 (2016) 493-504.
[49] J. Pagán, I. López, L. Aragonés, J. Garcia-Barba, The effects of the anthropic actions on the sandy beaches of Guardamar del Segura, Spain, Science of The Total Environment 601-602 (2017) 1364-1377.
[50] A. Sánchez-Arcilla, M. García-León, V. Gracia, R. Devoy, A. Stanica, J. Gault, Managing coastal environments under climate change: Pathways to adaptation, Science of The Total Environment 572 (2016) 1336-1352.
[51] Intergovernmental panel on climate change, Climate change 2014: synthesis report, IPCC Geneva, Switzerland, 2014.
[52] R. J. Bergillos, M. Ortega-Sánchez, M. A. Losada, Foreshore evolution of a mixed sand and gravel beach: The case of Playa

Granada (Southern Spain), in: Proceedings of the 8th Coastal Sediments, World Scientific, 2015.
[53] R. J. Bergillos, C. Rodríguez-Delgado, A. López-Ruiz, A. Millares,M. Ortega-Sánchez, M. A. Losada, Recent human-induced coastal changes in the Guadalfeo river deltaic system (southern Spain), in: Proceedings of the 36th IAHR World Congress.
[54] R. J. Bergillos, C. Rodríguez-Delgado, A. Millares, M. Ortega-Sánchez, M. A. Losada, Impact of river regulation on a Mediterranean delta: Assessment of managed versus unmanaged scenarios, Water Resources Research 52 (2016) 5132-5148.
[55] R. J. Bergillos, M. Ortega-Sánchez, G. Masselink, M. A. Losada, Morpho-sedimentary dynamics of a micro-tidal mixed sand and gravel beach, Playa Granada, southern Spain, Marine Geology 379 (2016) 28-38.
[56] R. J. Bergillos, A. López-Ruiz, M. Ortega-Sánchez, G. Masselink, M. A. Losada, Implications of delta retreat on wave propagation and longshore sediment transport-Guadalfeo case study (southern Spain), Marine Geology 382 (2016) 1-16.
[57] R. J. Bergillos, A. López-Ruiz, D. Principal-Gómez, M. Ortega-Sánchez, An integrated methodology to forecast the efficiency of nourishment strategies in eroding deltas, Science of The Total Environment 613-614 (2018) 1175-1184.
[58] R. J. Bergillos, C. Rodriguez-Delgado, G. Iglesias, Wave farm impacts on coastal flooding under sea-level rise: A case study in southern Spain, Science of The Total Environment 653 (2019) 1522-1531.
[59] R. Carballo, G. Iglesias, Wave farm impact based on realistic wave-WEC interaction, Energy 51 (2013) 216-229.
[60] L. Holthuijsen, N. Booij, R. Ris, A spectral wave model for the coastal zone, ASCE, 1993.
[61] R. T. McCall, G. Masselink, T. G. Poate, J. A. Roelvink, L. P. Almeida, M. Davidson, P. E. Russell, Modelling storm hydrodynamics on gravel beaches with XBeach-G, Coastal Engineering 91 (2014) 231-250.
[62] R. T. McCall, G. Masselink, T. G. Poate, J. A. Roelvink, L. P. Almeida, Modelling the morphodynamics of gravel beaches during storms with XBeach-G, Coastal Engineering 103 (2015) 52-66.
[63] R. J. Bergillos, G. Masselink, R. T. McCall, M. Ortega-Sánchez, Modelling overwash vulnerability along mixed sand-gravel coasts with XBeach- G: Case study of Playa Granada, southern Spain, in: Coastal Engineering Proceedings, volume 1, 2016, p. 13.
[64] R. J. Bergillos, G. Masselink, M. Ortega-Sánchez, Coupling cross-shore and longshore sediment transport to model storm response along a mixed sand-gravel coast under varying wave directions, Coastal Engineering 129 (2017) 93-104.
[65] Deltares, XBeach-G GUI 1.0. User Manual, Delft, The Netherlands, 2014.